2.C Time-Resolved Study of Surface Disordering of Pb(110)

Melting is one of the most common phase transformations; however, the process is not completely understood as no generally accepted theory exists to provide an understanding of this phenomenon on the atomic level. It is believed that melting is initiated at the surface of a material, at a temperature slightly below the bulk-melting temperature T_m.[1] This offers an understanding of the lack of parity between supercooling and superheating. A thin, disordered surface layer, formed below T_m, would act as a nucleus for melting into the bulk at T_m, thus precluding superheating. Several years ago, the formation of a disordered surface layer on Pb(110) was observed at temperatures below the bulk-melting point.[2] Since then, much work has been undertaken to characterize the thermally induced structural phase transformations that take place at solid surfaces.

Frenken *et al.* provided the first conclusive evidence of surface pre-melting (the formation of a thin, disordered surface layer below T_m).[2] Using the ion-shadowing and blocking technique, they showed that the Pb(110) surface exhibits a reversible order-disorder transition below the bulk-melting temperature (T_m = 600.7 K). These ion-shadowing and blocking results were also supported by a reflection high-energy electron diffraction (RHEED) study and infrared emissivity measurements on Pb(110) near T_m.[2] Further work with ion-shadowing and blocking revealed that the Pb(110) surface begins to disorder in the temperature range of 450–560 K and that the thickness of the disordered layer grows logarithmically in the range $0.3\ \text{K} \leq \Delta T \leq 40\ \text{K}$, where $\Delta T = T_m - T$.[3] This technique also revealed a change from logarithmic growth of the disordered-layer thickness to a power-law dependence for $\Delta T < 0.3$ K, which is attributed to the effect of long-range atomic interactions.[3] The pre-melting phenomenon depends on surface packing and, for Pb, is most pronounced for open surfaces such as (110), but is not observed for the close-packed (111) surface.[3]

X-ray photoelectron diffraction (XPD)[4] and low-energy electron diffraction[5] were also used to study surface pre-melting on Pb(110) and provided characteristic temperatures for the onset of surface disorder of 530±5 K and 543±3 K, respectively. Recently, an XPD study on Pb(100) revealed disordering behavior intermediate to that of Pb(110) and Pb(111).[6] X-ray scattering studies have also observed surface pre-melting on Pb(110).[7,8]

Molecular dynamics (MD) simulations dealing with the high-temperature behavior of metals have shown evidence for disordering below the bulk-melting temperature on Al(110),[9] Ni(110),[10] and Au(110).[11] However, these studies did not examine the time evolution of the disordering process. MD studies that deal with time evolution treat the behavior of metal surfaces above the thermodynamic melting point[12,13] as a distinctly different phenomenon than that of surface pre-melting. To our knowledge, currently

available MD studies on metals do not explicitly treat the temporal evolution of surface pre-melting.

There have been many time-resolved studies of laser-induced melting.[14] Picosecond transient reflectance measurements were used to examine the dynamics of the melting of Au and Cu.[15] Crystallization velocities as high as 100 m/s were observed, and it was proposed that the velocity for solidification in metals is limited by the speed of sound. It should be emphasized here that these studies involved bulk melting, that is, the occurrence of a first-order phase transformation. The work described here involves studying the dynamics of the formation of the disordered layer on Pb(110) at temperatures below T_m. This pre-melting phenomenon is different in that (1) it is a transformation that is continuous over some temperature range, (2) it is known to be reversible at low heating and cooling rates, and (3) it depends on surface structure.

Most of the time-resolved, laser-induced melting work employs classical transition-state theory,[16] which provides satisfactory agreement with experimental results. However, the experimental conditions for the work described here are quite different. First, in the case of surface pre-melting, unlike bulk melting, disordering of the surface occurs below the bulk-melting temperature. Indeed, the nature of the surface order-disorder transition has not been completely characterized. Much evidence suggests that the surface pre-melting phenomenon is a continuous process, as opposed to the abrupt first-order transition that occurs in bulk melting.[2,17] Secondly, the RHEED geometry allows us to probe depths of 10 Å or less. Coupling the surface sensitivity of RHEED with the much larger skin depth of the heating laser pulse (~140 Å in Pb for our experimental conditions) leads to a situation where the probed layers are isothermal to a good approximation. This is to be contrasted with other techniques such as transient reflectance or conductance, which typically probe depths of $\gtrsim$100 Å, where temperature gradients are significant. The interesting character of surface pre-melting leads us to study the nature of the disordered-layer growth and reordering processes. Here we report on a time-resolved study of the laser-induced disordering of Pb(110).

The method we use is picosecond RHEED.[18] A schematic diagram of the experimental setup is shown in Fig. 48.21. A picosecond laser pulse is split into two beams. The first beam induces a fast surface-temperature rise on the sample, while the second is incident on the cathode of a photoactivated electron gun, which produces a collimated electron pulse. The energy of the electron pulse in the work reported here was 18.2 keV, and its pulse width was determined by operating the picosecond electron gun as a streak camera,[18] and found to be ~180 ps measured at FWHM. The electron pulse is well synchronized with the heating-laser pulse and is used to generate a RHEED pattern of the surface of the sample. A RHEED pattern from a flat surface consists of a series of streaks or lines, whose separation can be related to the spacing of the atoms at the surface. Typically, each RHEED pattern is obtained by averaging several hundred shots, although single-shot operation

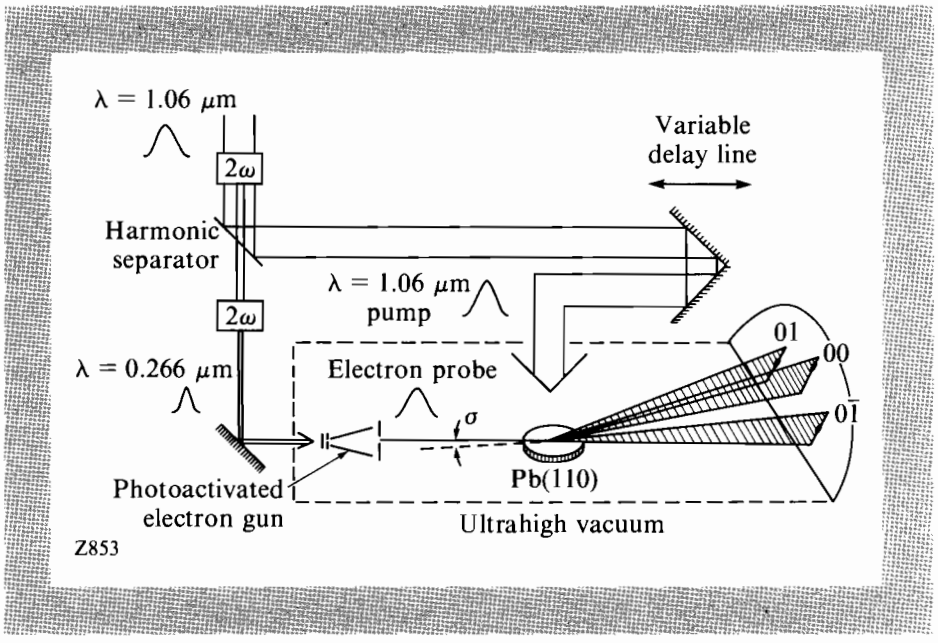

Fig. 48.21
Picosecond, time-resolved, reflection high-energy electron diffraction (RHEED). The laser pump and electron probe are well synchronized. The electron energy is 18.2 kV and the angle of incidence of the electron beam on the sample is ~3°.

was demonstrated to be feasible.[18] Time-resolved RHEED patterns can also be obtained, giving information on the structure and temperature of the surface at various times relative to the arrival of the heating-laser pulse. Prior to experiments, the sample is cleaned by cycles of Ar ion bombardment followed by annealing. Sample cleanliness is checked by Auger electron spectroscopy.

We have recently used the technique of picosecond RHEED to time-resolve the surface-temperature rise induced by a ~170-ps laser pulse incident on Pb(110).[18] This work dealt with the fast temperature rise induced on a surface that was initially at room temperature and undergoes no phase transformation. For studying the time-resolved dynamics of the surface-disordering process, the sample is biased at a temperature close to the temperature at which the surface begins to disorder. For the work reported here, the sample is biased at 487 K. The picosecond laser-heating pulse raises the surface temperature from the initial bias level to temperatures ranging from below to above the surface-disorder temperature. The time-resolved intensity of the RHEED streaks is then obtained for given time delays between the laser-heating pulse and the electron probe pulse.

The picosecond RHEED pattern is amplified using a microchannel plate (MCP) proximity focused to a phosphor screen, the output of which is lens coupled onto a linear array detector. Quantitative analysis proceeds by taking line scans through the recorded RHEED streaks. A shutter is placed in the path of the heating-laser beam such that every other pulse interacts with the sample, producing RHEED patterns with and without laser heating. The associated line scans are sorted and averaged in separate memories of the computer. Data analysis consists of comparing the peak heights of the laser-heated and unheated scans and generating a graph of I/I_0 versus time, where I and I_0 are the intensities through the center of the considered RHEED streak

corresponding to the laser-heated surface and the nonheated surface, respectively. The RHEED pattern was studied to ensure that the shape of the streaks remains unchanged with temperature. Thus, the measured intensity of a RHEED streak is directly related to the number of electrons scattered into it. For the experiments reported here, the angle of incidence of the pulsed electron beam is ~3°, resulting in a probe depth of ~3 monolayers, and the electron beam is incident along the [1$\bar{1}$2] azimuth.

The modulation of the streak intensity caused by laser heating is related to the surface temperature through a calibration obtained by static heating. The sample is heated on a resistively heated stage and the intensity of a streak is recorded as a function of the surface temperature, measured by a thermocouple mounted on the surface of the sample. This yields the normalized RHEED streak intensity when the sample is heated from the bias temperature to a given temperature. Results of this measurement are shown in Fig. 48.22. This measurement provides the means by which we can assign a temperature to a particular nonvanishing RHEED streak intensity. For $T \geq 540$ K, the elastically diffracted electron intensity becomes indistinguishable from the background, indicating the disordering of the probed surface layer. We thus define $T_d = 540$ K as the temperature at which our probed layer is disordered.

The experimentally determined time-resolved modulation of the RHEED streak intensity for various laser fluences is shown in Fig. 48.23. This is to be compared with the solid line, which is the calculated intensity modulation obtained by converting the output of a solution of the one-dimensional heat-diffusion model to an intensity modulation using the calibration in Fig. 48.22. The model is given by the equation

$$C\frac{dT(z,t)}{dt} = \mathrm{K}\frac{d^2T(z,t)}{dz^2} + I(1-R)\alpha e^{-\alpha z} f(t)^{-8.5},$$

where $T(z, t)$ is the temperature profile at distance z normal to the surface ($z = 0$), t is time, $f(t)$ is the temporal dependence of the laser pulse, which is assumed Gaussian, $C = 1.58 \times 10^6$ J/m^3 K is the heat capacity per unit volume,[19] K = 32.2 W/m K is the thermal conductivity,[19] $R = 0.81$ is the reflectivity,[20] $\alpha = 7.05 \times 10^7$ m^{-1} is the absorption coefficient,[20] and I is the peak laser intensity in W/cm^2. For reference, the right side of the intensity-modulation graphs give the surface temperature obtained from the calibration in Fig. 48.22.

We next discuss the time-resolved heating and disordering results. In Figs. 48.23(a) and 48.23(b), the laser fluence is set so as to heat the surface to temperatures less than T_d. A solution of the heat-diffusion model for Figs. 48.23(a) and 48.23(b) gives peak surface temperatures of 523 K and 537 K, respectively. We then heated the surface with laser fluences sufficient to raise the surface temperature above T_d as shown in Figs. 48.23(c) and 48.23(d). A solution of the heat-diffusion model for the case in Fig. 48.23(c) indicates that the surface temperature is raised to ~558 K, approximately 18 K above T_d. A solution of the model for the case in Fig. 48.23(d) predicts

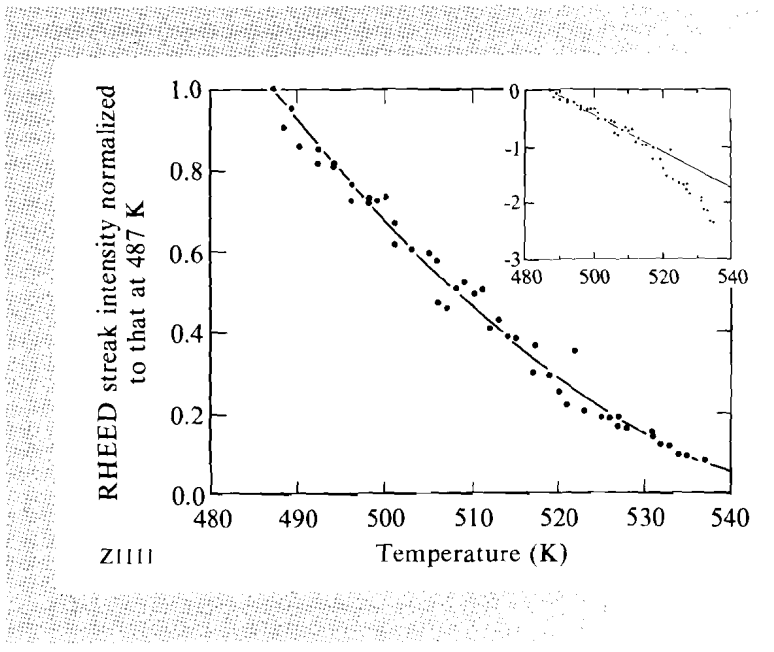

Fig. 48.22
RHEED streak intensity versus sample temperature normalized to the streak intensity at the sample bias temperature of 487 K. The sample is heated on a resistively heated stage and the temperature is measured using a thermocouple attached to the surface. The location of the line scan across the diffraction pattern is the same as that for a pulsed laser heating experiment. A curve fit is made to the data and is used in conjunction with the heat-diffusion model to obtain the predicted time-resolved modulation of the RHEED streak intensity in Fig. 48.23. In the inset, the RHEED streak intensity is plotted on a logarithmic scale. The line fit includes data points up to that which maximizes the linear correlation.

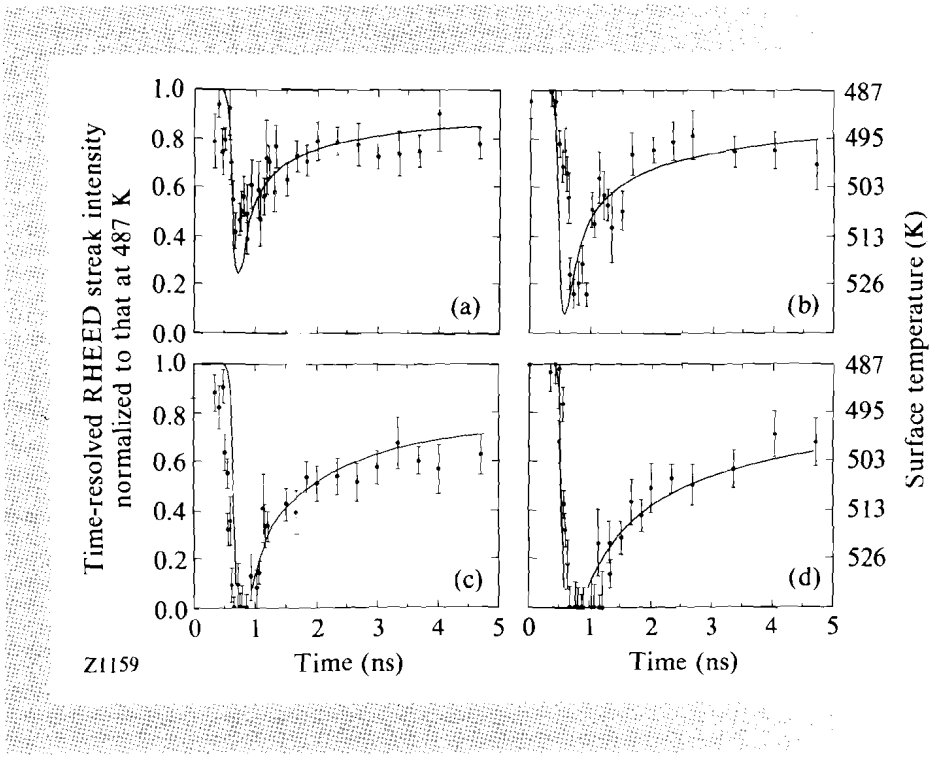

Fig. 48.23
Transient modulation of RHEED streak intensity and surface temperature on Pb(110) irradiated with Nd:YAG ($\lambda = 1.06$ μm) laser pulses of varying peak intensities: (a) 1.4×10^7 W/cm^2, 165-ps FWHM; (b) 2.0×10^7 W/cm^2, 163-ps FWHM; (c) 2.7×10^7 W/cm^2, 173-ps FWHM; (d) 3.6×10^7 W/cm^2, 171-ps FWHM. In (c) and (d), the normalized streak intensity disappears for some time corresponding to a transient disordering of the probed surface layer. The reappearance of the streak intensity indicates the subsequent reordering of the surface.

a surface temperature rise to ~581 K, approximately 41 K above T_d. The two fluences were chosen to explore the possible dependence of the disordering dynamics on overheating above T_d. In both cases, there exists some time where we are unable to detect RHEED streaks, corresponding to the elastically diffracted electrons, indicating that the probed surface region (~3 monolayers) is disordered. The time for which the streaks vanish depends on the level of overheating above T_d and is found to be ~200 ps for Fig. 48.23(c) and ~500 ps for Fig. 48.23(d). This is followed by the reappearance of the RHEED streaks as the surface cools and reorders. In all the graphs, the streak intensity is normalized to that at the bias temperature of 487 K. In Figs. 48.23(c) and 48.23(d), the results of the model are truncated since the static calibration, which allows us to convert the solution of the heat-diffusion model to an intensity modulation, could not detect the RHEED streaks above ~540 K.

The error bars in Fig. 48.23 give the uncertainty of the streak intensity modulation and are mainly due to MCP noise. Other sources of errors in our measured intensity modulation include the spatial nonuniformity of the heating-laser profile on the surface, which is measured to be ±12% across the surface, and the stability of our laser. Shot-to-shot laser fluctuations and long-term stability of the electron probe are compensated for by normalization and averaging. The heating-laser stability is regularly monitored during the experiment and is maintained to better than 10%. Our time-resolved measurements are the result of the convolution of the electron probing pulse with the actual temporal profile of the surface temperature. Such convolution effects, which are not included in our analysis, are most significant for times near the minimum of the normalized RHEED streak intensity where the rate of change of temperature with time is greatest. The absolute timing between the electron probe pulse and the laser-heating pulse is not experimentally determined. The temporal position of the theoretical streak-intensity modulations in Fig. 48.23 is set by minimizing the mean-square difference between the experimental results and the theory. For Figs. 48.23(a)–48.23(c), this minimization is performed for times between 1 and 2 ns, while for Fig. 48.23(d) it is performed between 1.3 and 3.3 ns. Taking the previous convolution effects into consideration, the sets in Figs. 48.23(a) and 48.23(b) show good agreement with the classical heat-diffusion model. In these sets, the laser fluence is kept below the fluence necessary for surface disordering.

The time-resolved modulation of the RHEED streak intensity for laser fluences above the surface disorder fluence again shows a good fit to that predicted from the classical heat-diffusion model. Observation of the actual growth of a disordered-surface region would result in a deviation between the experimentally determined, time-resolved intensity modulation and that predicted by classical heat diffusion. For example, a discrepancy in the time at which I/I_0 vanishes could reflect the time required to nucleate and grow the disordered surface layers. However, with the present time resolution, this is not observed. This indicates that, although we have achieved laser-induced disordering of the surface, we are unable to observe the growth of the disordered layer with the present time resolution of our experiment. After

disordering, the normalized RHEED streaks reappear and their intensity agrees well with theoretical predictions. We conclude that the regrowth of crystalline order occurs in a time scale shorter than our time resolution. These results imply that the disordering and regrowth of the probed surface layer each occur in a time scale shorter than the pulse width of our electron probe.

In conclusion, using time-resolved RHEED, we have observed laser-induced surface disordering on Pb(110). Furthermore, this transformation is observed to be completely reversible within the time resolution of our experiment. This is significant since, previously, surface disordering has only been studied using conventional static surface probes. Here, we extend those measurements to heating and cooling rates of the order of 10^{11} K/s. Finally, the actual growth of the disordered layer and the regrowth of surface order were not observed. We conclude from this that the times necessary to disorder and regrow the probed surface layer are each shorter than the pulse width of our electron probe (~180 ps).

ACKNOWLEDGMENT

This work was supported by the U.S. Department of Energy under contract No. DE-FG02-88ER45376. Additional support was provided by the Laser Fusion Feasibility Project at the Laboratory for Laser Energetics, which is sponsored by the New York State Energy Research and Development Authority and the University of Rochester. We gratefully acknowledge E. A. Murphy for her assistance with the experiments.

REFERENCES

1. G. Tammann, *Zeitschr. Phys. Chem.* **72**, 609 (1910).
2. J. W. M. Frenken and J. F. van der Veen, *Phys. Rev. Lett.* **54**, 134 (1985); J. W. M. Frenken, P. M. J. Maree, and J. F. van der Veen, *Phys. Rev. B* **34**, 7506 (1986).
3. B. Pluis *et al.*, *Phys. Rev. B* **40**, 1353 (1989); B. Pluis *et al.*, *Surf. Sci.* **239**, 265 (1990); B. Pluis, D. Frenkel, and J. F. van der Veen, *Surf. Sci.* **239**, 282 (1990).
4. U. Breuer, O. Knauff, and H. P. Bonzel, *Phys. Rev. B* **41**, 10848 (1990); *J. Vac. Sci. Technol. A* **8**, 2489 (1990).
5. K. C. Prince, U. Breuer, and H. P. Bonzel, *Phys. Rev. Lett.* **60**, 1146 (1988); U. Breuer *et al.*, *Surf. Sci.* **223**, 258 (1989).
6. E. A. Murphy, H. E. Elsayed-Ali, K. T. Park, J. Cao, and Y. Gao, *Phys. Rev. B* **43**, 12615 (1991).
7. P. H. Fuoss, L. J. Norton, and S. Brennan, *Phys. Rev. Lett.* **60**, 2046 (1988).
8. B. Pluis *et al.*, *Surf. Sci.* **222**, L845 (1989).
9. P. Stoltze, J. K. Nørskov, and U. Landman, *Phys. Rev. Lett.* **61**, 440 (1988); *Surf. Sci.* **220**, L693 (1989); P. Stoltze, *J. Chem. Phys.* **92**, 6306 (1990).